A Recording Microfluorospectrophotometer

The instrument permits analysis *in situ* of porphyrin and other autofluorescing substances in tissues.

Walter J. Runge

Substances responsible for autofluorescence in tissue are usually identified, after suitable purification, by comparison of their fluorescence spectra and other properties with those of reference compounds. Fluorescence microscopy reveals cytological and histological patterns of fluorescence distribution, but the visualized fluorescence has a heterogeneous origin which is, at best, only partially clarified by chemical extraction and analysis. Spectral analysis of histofluorescence is of unique value since it offers precise information of component fluorescence materials. Though fluorescence spectrometry is being employed increasingly in other areas, it has been used in relatively few studies of tissue fluorescence (*1–4*). The published results have been obtained with either photographic recording of the spectra or visual measurement of the emission bands. However, an electronic recording instrument offers a number of advantages over the more usual techniques of histofluorescence spectrometry.

In histologic preparations containing autofluorescing structures, the maximum light intensities are very low (*3*). Under appropriate conditions, photographic emulsions permit prolonged exposure for integration of these low radiant energies. The photographic method, satisfactory for compounds which are stable to the exciting light, is inappropriate when there is noticeable "photo-fading" of the fluorescence, as in the case of vitamin A and porphyrins.

The purpose of this article is to describe a recording electronic microfluorospectrophotometer that has been developed with special reference to the study of tissue porphyrins. Work in this laboratory on fluorescence spectra of cellular porphyrins began in 1948 with the acquisition of a Steinheil Universal microspectrograph of the type Borst and Königsdörffer employed in their well-known work on tissue porphyrins in congenital porphyria (*1*). The initial objective was to record spectra photographically, but the photo-fading effect necessitated a faster recording system. This need led us to undertake the development of an instrument by which spectra can be recorded electronically. [Other models were built and tested by P. Maseley, L. P. Christenson, and G. R. Price between 1949 and 1955; a brief discussion of one of these units was given in 1955 (*5*).]

The primary goal was to record porphyrin fluorescence spectra from various tissue structures, including individual cells or nuclei, excited to autofluorescence under a fluorescence microscope and observed at various magnifications, according to the size of fluorescing structures, which might vary from $\sim$ 1.0 to 10^{-3} millimeter. Some fluorescing objects showed fading or color shift or both upon brief ($<$1.2 minutes) exposure to the exciting light. Since spectral resolution of at least 20 angstroms at 6400 angstroms seemed essential, the spectral range from 5800 to 7000 angstroms had to be scanned at a rate of at least 20 angstroms per second. The radiant energies ($<10^{-12}$ watts) of various porphyrin-containing fluorescing elements of tissues were estimated from the exposure times (1.5 to $\sim$ 6 minutes) which were necessary to obtain a photograph of normal density on high-speed Ektachrome film (daylight type). A detailed discussion of criteria for the design of the instrument may be found elsewhere (*6–8*).

General Description

The general appearance and principal components of the microfluorospectrophotometer are shown in Figs. 1 and 2, and further details are given in Table 1. The light source (HG in Figs. 1 and 2), an Osram HBO 200 W-L2, operates in a Zeiss spherical microscope lamp housing. The power comes from a regulated d-c-supply (H_gP) that can be operated in either "constant current" or "constant voltage" mode (*9*), by controlling the arc current with a current-sensitive series resistance or by stabilizing the lamp radiation with a shunt-series thermionic valve regulator, which is actuated by a change in light output with a photo cell in a selected spectral range. The mercury light passes through a 50-millimeter cooling-cuvette (F_c) before being interrupted by a sealed chopper (C) which is rotated with a synchronous motor over a step-up gear. Neon or argon glow lamps (GL) can be positioned at the quartz entrance window for calibration of spectral wavelength. Mercury light for fluorescence excitation is obtained with filters (F) after chopper modulation, which provides a maximum irradiance of 4×10^4 erg/cm^2 sec. Normal operation requires 7×10^3 erg/cm^2 sec.

The filter combination (F_c = 50 mm, 10 percent $CuSO_4$; + Corning 5030, CS 5-57; + Schott BG 38, 1 mm; + Schott BG 12, 1 mm; + Corning 5113, CS 5-58; + Bausch and Lomb Interference Filter 405) passes light of 4050 $\pm$ 50 Å. The microscope is a Leitz SM-POL stand, carrying a special monocular tube (*10*) with a prism deflector that makes possible either spectral measurement or visual observation. The lengths of optical tubes for both types of work are equalized for Zeiss Neofluoar objectives. Secondary filters (F_s) are introduced into the beam in the compensator compartment of the microscope stand.

Spectral dispersion of the light emission from the specimen is achieved with the Steinheil Universal microspectrograph (*1, 11*) adapted to photoelectric readout in the conventional manner by addition of a projecting lens (L_p), a scanning mirror ($D_\lambda M$), and an exit slit (S_2). The exit slit is adjusted by air pressure (*12*). The preamplifier chassis (A) is bolted to an insulated box (B), which contains a photomultiplier (TD in Fig. 2*B*) in a shielded, refrigerated, thermally insulated housing. The photomultiplier operates at -18.5°C; this temperature is maintained with a Freon condensing unit (REF). The multiplier load, in separate

The author is a research associate in the department of medicine, Universiy of Minnesota, Minneapolis.

shielding, is also placed in the insulated box (Fig. 2*B*). The preamplifier output can be monitored with the oscilloscope. The signal voltage is brought into the rack by cable. The amplitude of the signal to be recorded can be adjusted to 100 percent with the gain control (G, Fig. 1). A meter (M) displays the signal level. A dial (W) permits manual adjustment of the wavelength, which can also be changed automatically by the motor that turns the chart paper.

The upper portion of the rack contains the high-voltage battery (HV) and the resistive bleeder chain of the photomultiplier and some potentiometers of the drive system of the spectrum scanner.

Not shown in the photograph are the regulated d-c filament supply, the central plate voltage supply (modified; see *13*), a servo power amplifier (modified; see *14*), and the readout system. Ground transfer methods (*15*) are used in the electronic and electrical systems.

Design Principles

The design of the microfluorospectrophotometer is more easily demonstrated by separating the data-generating system from the data-recording system (Fig. 2).

In the data-generating system exciting light from a d-c–operated mercury arc (HG, Fig. 2*B*) isolated by a filter monochromator (F_c + F) is projected by the microscope condenser M_c into the specimen plane to form real monochromatic images of the circular apertures (C_a) in the revolving disk (C) after upward deflection with a front-surface mirror M_M. Fluorescent light is collected by the microscopic objective (M_o and brought to focus in its intermediate image plane. Rays emanating from this real image are parallel for all practical purposes (angular sinus ~ 0.01) and thus suited for spectral dispersion with any spectral apparatus whose entrance slit (S_1) is positioned in this plane. When so positioned, the slit will act as field diaphragm. Thus, length and width of the slit isolate the area covered in the object. The desired spectral resolution defines the adjustable slit width, and the slit length can be adjusted to fit the lateral extension of the fluorescing object.

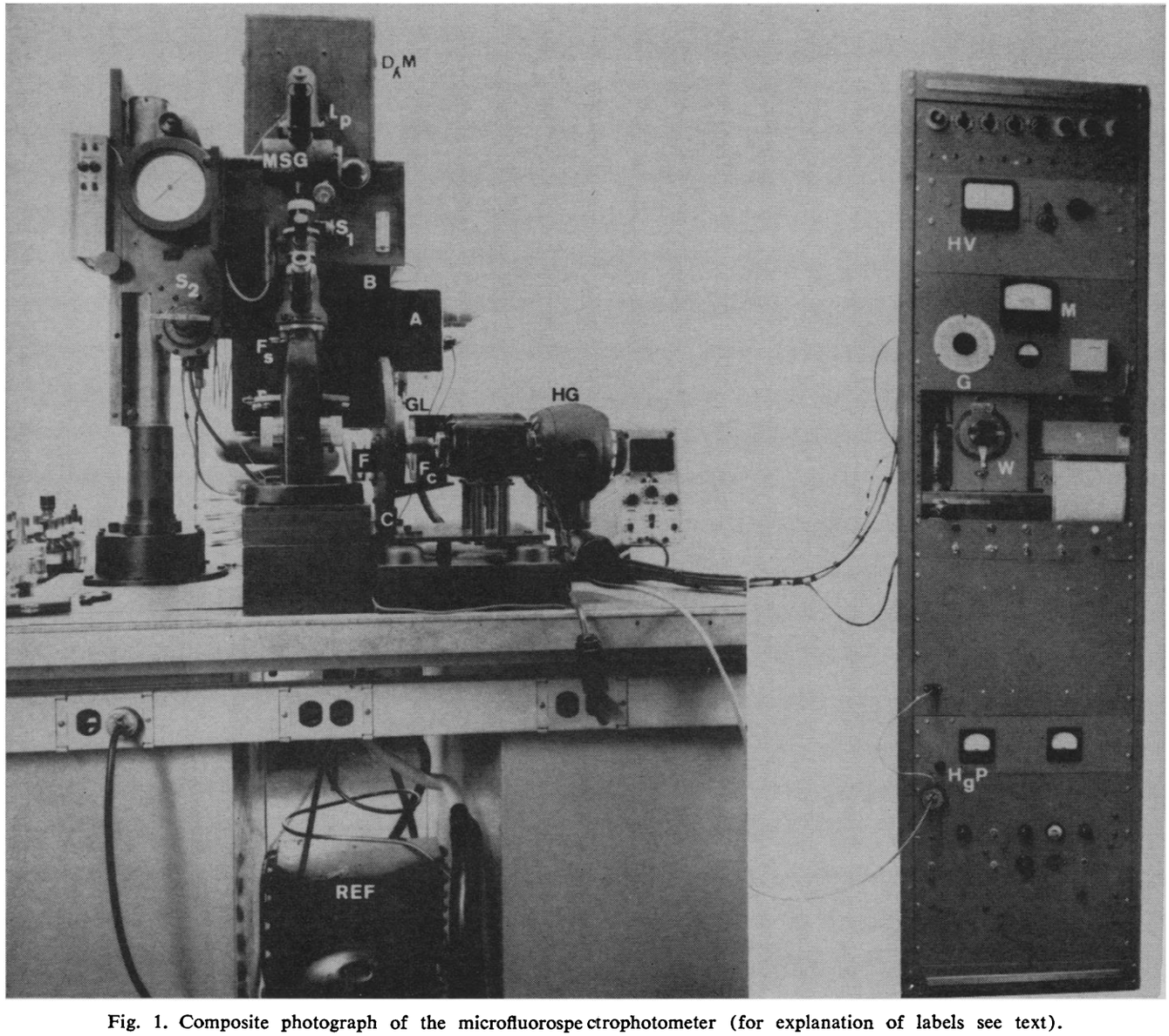

Fig. 1. Composite photograph of the microfluorospectrophotometer (for explanation of labels see text).

The isolated bundle of light, after passing through a collimating lens (L_c), is dispersed by a "minimum-deviation type" glass prism (P), and the resulting spectrum is accepted by the data-recording system.

The spectrum is projected onto the exit slit (S_2) with L_p (Fig. 2*B*) after downward deflection by mirror $D_\lambda M$. The angular deviation of the beam is varied by tilting the mirror mount sinusoidally and thus moving the spectrum across the exit slit. A condensing lens L_{co} focuses the jaws of slit S_2 on the photocathode (S20) of the photomultiplier.

Design Philosophy

In general, the limit of detection of very low levels of steady radiant energy depends entirely on the achievable signal-to-noise ratio (S_N) with a low dark current photomultiplier of maximum sensitivity, in conjunction with the

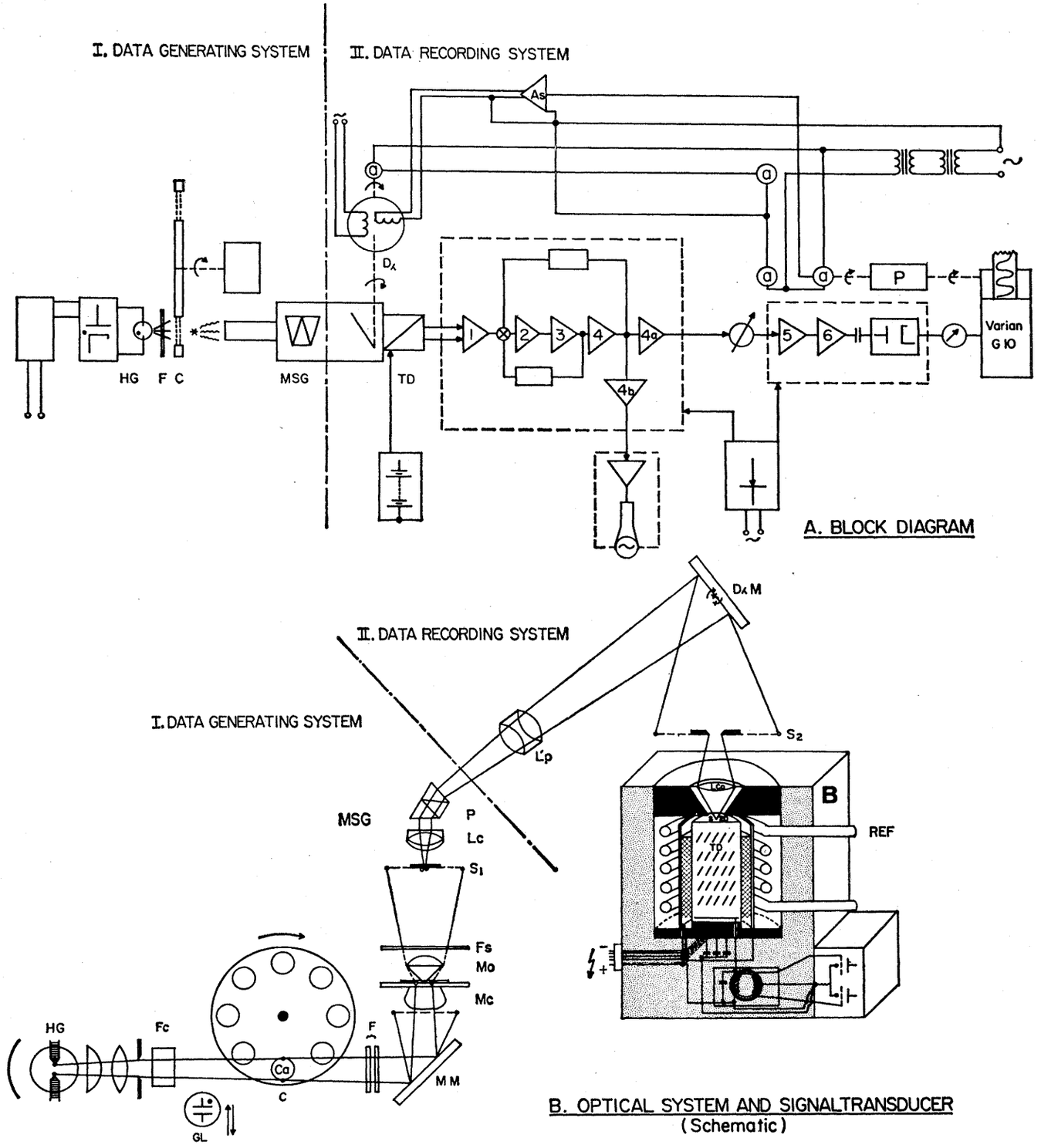

Fig. 2. Schematic diagram of the microfluorospectrophotometer (for explanation of labels see text).

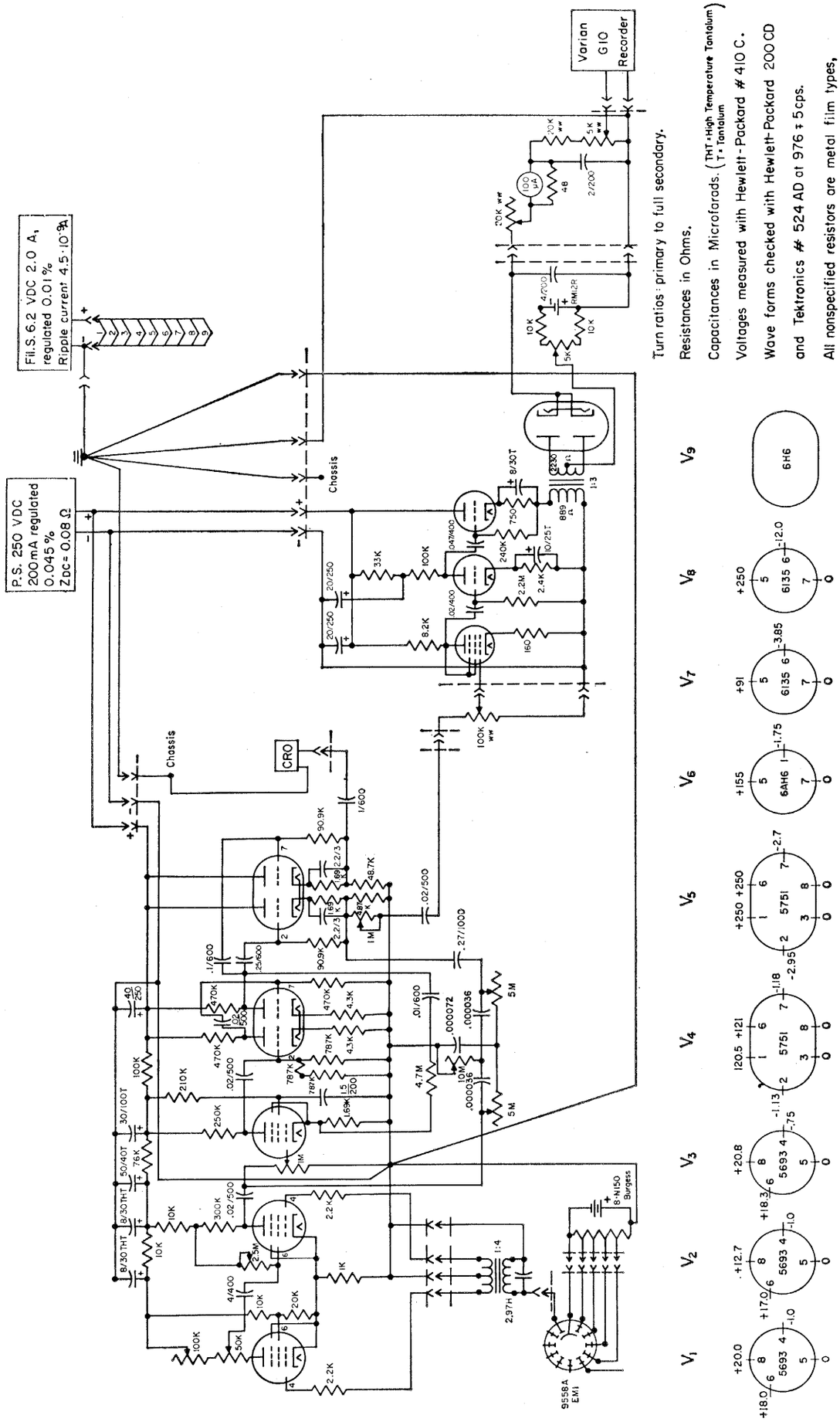

Fig. 3. Schematic diagram of the electronic amplifier chain of the microfluorospectro photometer.

type of the plate load and noise contribution of subsequent voltage amplifier stages. The root-mean-square noise-current of the anode of a photomultiplier is represented in close approximation (*6*) by:

$$[(<I_p^2>_{av})_{\Delta f}]^{\frac{1}{2}} = \mu\,[2e\,\Delta f(i_t + i_p)]^{\frac{1}{2}} \quad (1)$$

where I_p is the plate current, Δf is the band width, μ is the amplification factor, e is the electron charge, i_t is the thermionic cathode current, i_p is the signal cathode current, and the output current is

$$I_p = \mu \cdot i_p \quad (2)$$

Dividing Eq. 2 by Eq. 1 gives

$$S_N = \left[\frac{i_p^2}{2e\,\Delta f\,(i_t + i_p)}\right]^{\frac{1}{2}} \quad (3)$$

Equation 3 suggests that, given a highly sensitive photocathode, once the thermionic dark current i_t has been suppressed, a significant improvement in detectability can be expected only from a decrease in the band width (Δf) of measurements.

The noise in a number of different light-detecting circuits employing photomultiplier tubes was analyzed. It became apparent in this study that in histofluorescence spectrometry a useful limit of detectability is not approached by the conventional technics of choosing an optimum size for the photocathode (*4*), using very high values for the plate-load resistance, measuring with a narrow band-pass system, or by a combination of any of these. Cooling of the photomultiplier cathodes reduced their quantum efficiency at temperatures lower than −20°C.

Another factor had to be taken into consideration, that in tissue autofluorescence the emission of fluorescence is very unsteady, especially at low intensities. This problem presents itself as high "noise in signal" when intensity of fluorescence is measured with photomultipliers. Any fluorescing compound present in tissues is expected to have more than one time constant of fluorescence, depending on the structure in which it occurs. The theoretical solution of the noise-in-signal problem which follows emphasizes the dominant role of the load circuit configuration of the photomultiplier.

The emission of fluorescent light is governed by the exponential rule

$$dN = \frac{N}{T_0} \exp\left(-\frac{t}{T_0}\right) dt,$$

where N represents the emitted photons

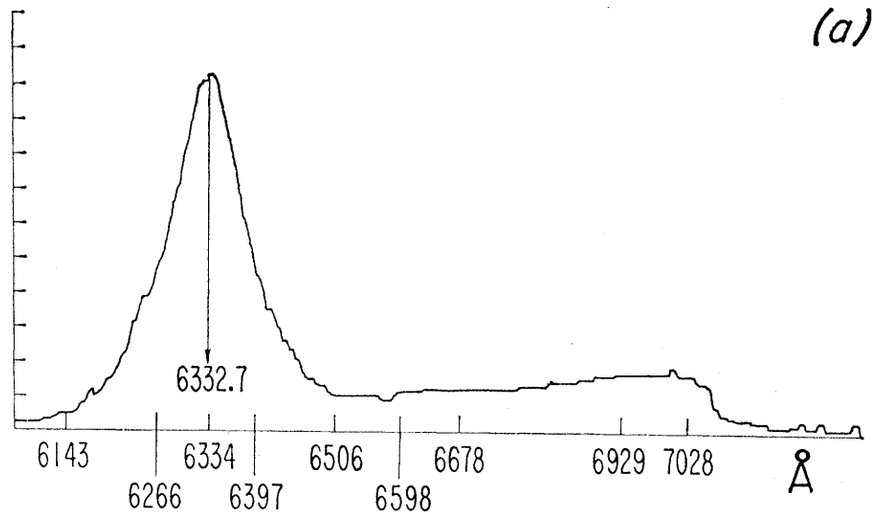

Fig. 4. Fluorescence spectra of porphyrins as shown by the microfluorospectrophotometer. (*a*) Protoporphyrin-IX-dimethylester (10^{-10} g) solubilized in aqueous 5-percent sodium lauryl sulfate adjusted with HCl to *p*H 6.6 (see Fig. 4, *b–g*, on following two pages).

and T_0 is the time constant of fluorescence. If the cathode-to-plate transit time is neglected, the quantity of electricity dq which arrives at the photomultiplier plate during the time dt can be estimated as

$$dq = \frac{Q}{T_0} \exp\left(-\frac{t}{T_0}\right) dt$$

with Q representing the charge in the parallel circuit of total plate capacitance and plate resistance. The expression yields as plate current

$$I_p = \frac{dq}{dt} = \frac{Q}{T_0} \exp\left(-\frac{t}{T_0}\right)$$

In the plate-load circuit, this current is

$$I_p = i_R(t) + i_C(t)$$

where $i_R(t)$ is the current through the

Table 1. Characteristics of the microfluorospectrophotometer.

Component and characteristic	Value
Photomultiplier	
Type	EMI No. 9558A
Spectral response of cathode	S20 (nominal)
Decrement of spectral response Ref: 6266- to 6678-Å range	−10 percent at 6929 Å; −63 percent at 7028 Å
Supply voltage	1.5 kv
Bleeder-current	9.8×10^{-4} amp
d-c—dark current	10^{-9} amp at 20°C; 1.5×10^{-10} amp at −18.5°C
Plate noise current 976 ± 10 cy/sec, −18.5°C	$\sim 10^{-15}$ amp
Quantum efficiency at 6400 Å	< 10 percent
Plate sensitivity at 6400 Å and −18.5°C	4.2×10^{-2} amp/watt
Plate-load transformer	
Toroid type S3412 (*21*)	
Primary inductance	2.97 henry
Primary resistance	100 ohm (untuned)
Primary figure of merit	75
Shielding	180 db
Load impedance at signal frequency	$\sim 5 \times 10^8$ ohm
Bandwidth (tuned)	976 ± 10 cy/sec
Response time, $\frac{1}{2}/\Delta f$	~ 0.05 sec
Preamplifier	
Sensitivity	7×10^{-6} volt (peak to peak)
Equivalent noise input	4×10^{-6} volt (peak to peak)
Band pass	976 ± 20 cy/sec
Amplifier-chain	
Total gain (with feedback)	3.5×10^5
Recorder	
Type: Varian G 10	100 mv d-c, fixed span
Scanning range	4000 to 7050 Å
Scanning rate	2 to 100 Å/sec, adjustable (linear)

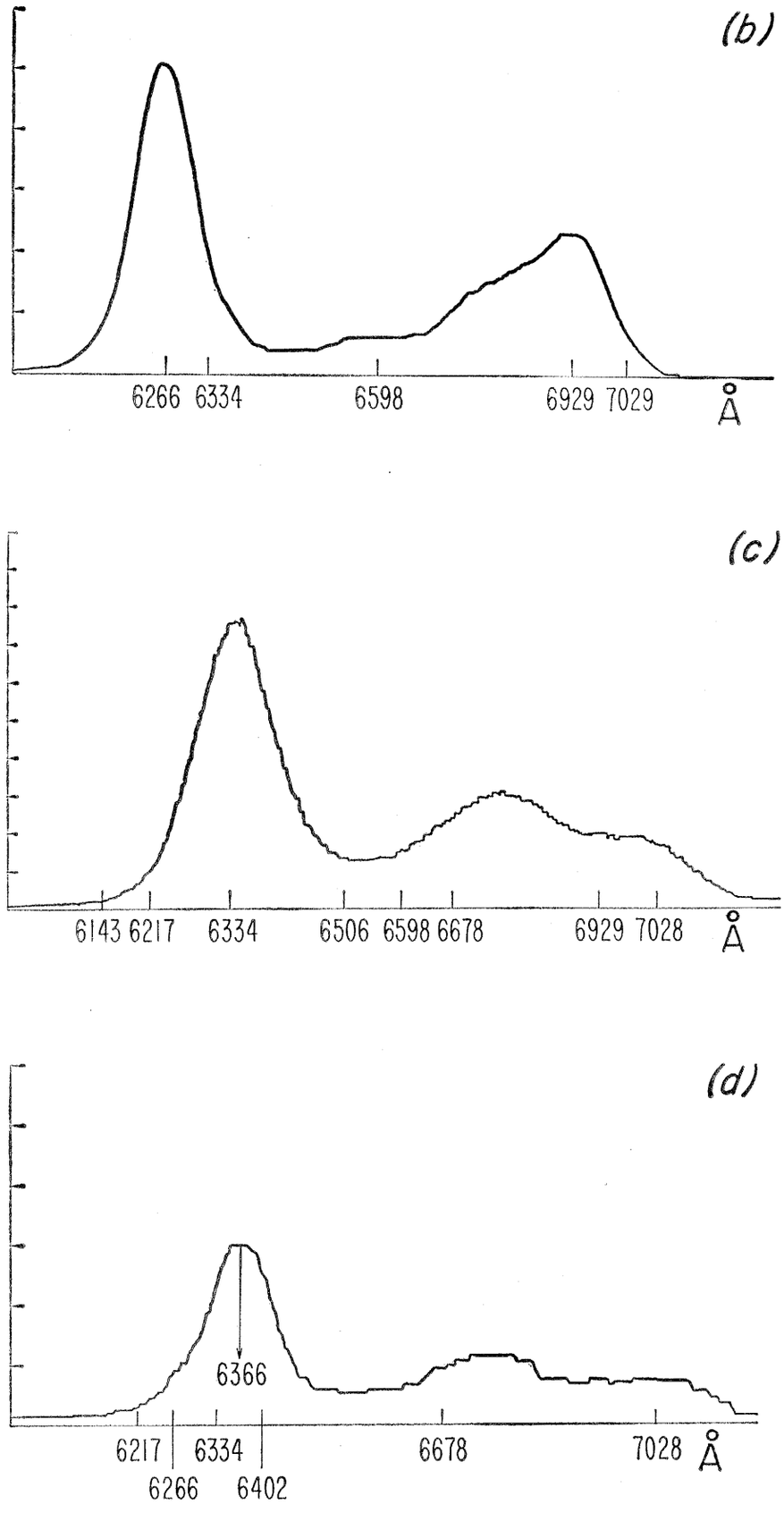

Fig. 4, *b–d*. (*b*) Uroporphyrin-I-octamethylester (10^{-9} g/ml) dissolved in a mixture of pyridine and glycerine (3:1 by volume). (*c*) Harderian gland of rat, 6-μ fresh frozen section, mounted in pyridine glycerine (3:1). Fluorescence was emitted from cytoplasm of acinar cells. (*d*) Cells from duodenal epithelium of a mouse which had been fed griseofulvin (6-μ fresh frozen section mounted in 0.01*N* HCl).

load resistor as a function of time, and $i_C(t)$ is the current through the shunt capacitance, C_p, as a function of time. If V is the output voltage across the plate load and R is the resistance, then

$$\frac{V}{R} + C_p \frac{dv}{dt} = \frac{Q}{T_0} \exp\left(-\frac{t}{T_0}\right).$$

By integration, and by introduction of the time constant of the plate load $T_1 = RC_p$, it is found that

$$V = \frac{Q}{C_p} \frac{T_1}{T_0 - T_1}\left[\exp\left(-\frac{t}{T_0}\right) - \exp\left(-\frac{t}{T_1}\right)\right];$$

thus the voltage-fluctuation becomes a direct function of T_0 and T_1. Since T_0 is fixed, V depends only on T_1. In order to make the result independent of T_0, T_0 is set equal to unity. The introduction of $T_1 = kT_0$ and $t = xT_0$, in above equation, then gives

$$V_x = \frac{Q}{C_p} \frac{k}{1-k} \times \exp(-x)\left\{1 - \exp\left[-x\left(\frac{1-k}{k}\right)\right]\right\}$$

where $k = T_1/T_0$. For the one condition $k = \infty$, the maximum voltage amplitude can be expected, as C_p can no longer discharge.

The maximum signal-to-noise ratio, however, cannot be obtained with $k = \infty$. When $k = 1$ ($T_0 = T_1$), the voltage is reduced to

$$V = \frac{Q}{C_p} \frac{t}{T_0} \exp\left(-\frac{t}{T_0}\right),$$

and the theoretical optimum ratio is achieved. The maximum value of this voltage pulsation

$$V_{max} = \frac{Q}{C_p} \frac{1}{e}$$

is reached in the period T_0. For values of $k = 10$ and $k = 10^{-1}$ the signal-to-noise ratio rapidly decreases to 60 percent of the optimum.

These calculations suggest that a tuned load impedance which resonates either at the frequency of the fluorescence emission or at a chopping or modulation frequency of the exciting energy should be used. Chopping the exciting light permits excellent control over the timing of the events of fluorescence. From above calculations it can be concluded that for the least noisy signal at maximum voltage amplitude, frequency of excitation, type of the tuned photomultiplier-plate load, fluorescence time constant, and period of the exciting pulse are interrelated.

The chopping frequencies for the theoretical optimum signal-to-noise ratio are too high to be practical for instrumentation (*16*). A feasible way of obtaining the least noisy signal with parallel tuned inductance-capacitance plate loads was found experimentally by generating fluorescence with pulses of exciting light in which the exciting period was about 10^2 times the average fluorescence time constant $\bar{T}_0$, which for free protoporphyrin in the Harderian gland was about 10^{-5} second. The high plate impedance of the photomultiplier when the plate current, I_p, is very small will not seriously affect the band-pass characteristics of the tuned circuit, and the contribution of the photomultiplier plate to the noise will be limited to

$$E_{p\ noise} \simeq \int_{f_1}^{f_2} I_p Z_{fo}$$

where $E_{p\ noise}$ is the total noise voltage across the photomultiplier plate load and Z_{fo} is the impedance at resonance. A pulsating current is generated at a photocathode if the light is interrupted by a disc in which there are n evenly spaced bridges and circular openings and which revolves at constant rate (meters per second). Depending on the actual optical imagery (Fig. 2*A*) and on the ratio, a, of the diameter of the hole to the circumference of the disc, the wave function

$$T/2 = r + s;\ r = 0.5\ at;\ s = T/2 - r$$

was determined for the exciting light: $T/2$ is the pulse duration, r is the period of rise, s is the period of decline, and t is variable time. Since the pulse time of this wave pattern is about 10^{-3} second, the duration of the excited fluorescence state of free tissue porphyrins ($\sim 10^{-5}$ second) tends to adjust the period of decline to the period of rise; the pulsating fluorescence signal as seen by the photocathode acquires already a clean quasi half-sine wave shape.

Signals with such a wave form can be conveniently handled. Loading of the photomultiplier plate with a nonterminated, primary-tuned transformer results in a sine-wave output voltage around the center-tapped primary winding.

The microfluorospectrophotometer uses this type of photomultiplier operation, as demonstrated in Fig. 3. The double-ended transformer output is directly connected to the grids of a specially designed differential input stage, operating under "starved current" (*8*) conditions. This amplifier uses pentodes

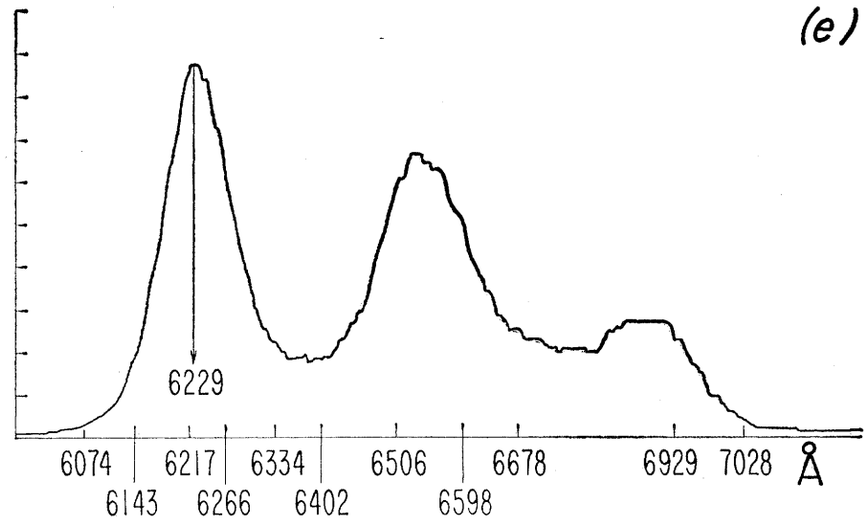

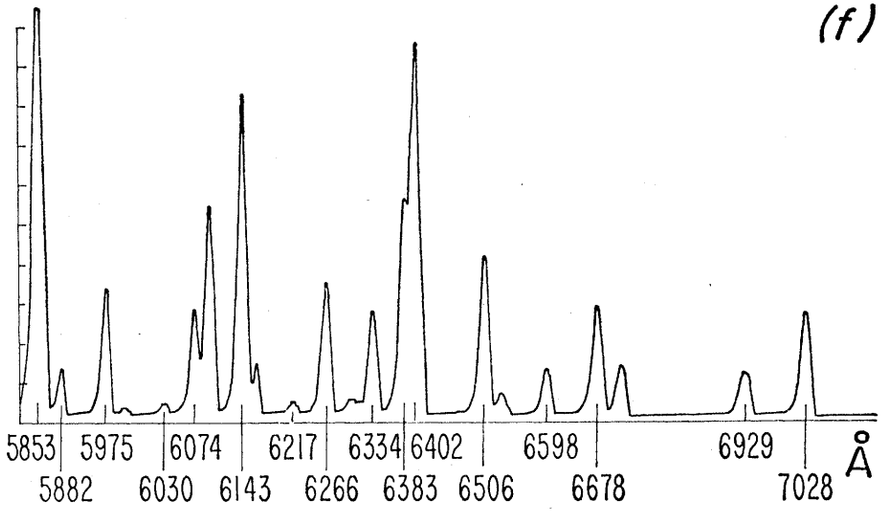

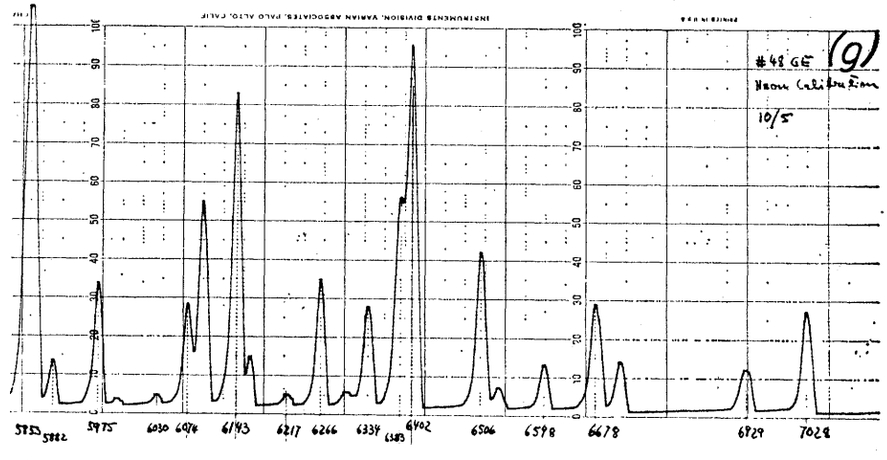

Fig. 4, *e–g*. (*e*) Rat liver cell (cytoplasmic area 10 μ^2; 6-μ fresh frozen section, mounted in pyridine glycerine (3:1); coproporphyrin I-ammonium salt (0.0005 g in 0.9-percent NaCl) had been injected intraportally 5 minutes before the rat was killed. (*f*) Discharge spectrum of a Neon Glow Lamp GE No. 48; slit width 2 μ as in *e*. Graphs *a–f* have been redrawn. (*g*) The graph shown in *f*, as originally produced by the microfluorospectrophotometer. All spectra were recorded with the same scanning speed (gear 10/5) at 20 Å/sec. Differences in scale are results of reproduction.

instead of triodes and achieves a far better common mode rejection than classical single-ended triode differential amplifiers. The phase reversal between the different electrodes of the pentode in relation to the phase angle of the fundamental signal component is used to achieve extremely high rejection for common inputs at the screen grid of the loaded tube (V_2).

Figure 3 also shows the remaining amplifier stages; a tuned negative feedback is employed over three stages. More than adequate gain (Table 1) is provided to drive the pen recorder after rectification of the alternating output voltage with a full wave diode circuit.

The speed of the recorder-paper drive (P) in Fig. 2*A* and the drive motor (D_λ) for the mirror ($D_\lambda M$) of the spectrum scanner are electrically coupled through a follow-up servosystem. The control voltage to the two-phase induction motor (D_λ) is varied with a nonlinear potentiometer bridge. Thus the speed at which the spectrum can be scanned decreases with the reduction of the spectral dispersion of the glass prism toward the red and provides the required resolution at 6400 Å. In order to obtain a linear representation of wavelength on the chart, an attempt (*17*) was made to fit the nonlinear characteristic of the potentiometer bridge to the nonlinear dispersion of the prism, but this proved to be impractical for any permanent calibration within 5 Å, even for short periods.

Presently the wavelengths of fluorescence spectra are determined from neon spectral lines recorded prior to the analysis of the fluorescing specimen.

Results

The apparatus as described has been used to locate and identify porphyrins in tissues, individual cells, and substructures of cells in a variety of histologic preparations as well as in microsamples of dissolved phycobilin and phycocyanin (*18*) and porphyrins. Some results obtained with the microfluorospectrophotometer are shown in Fig. 4 (*a–f* have been redrawn). The apparatus has been used to reveal the fluorescence spectra of protoporphyrin IX-dimethylester solubilized (*19*) in sodium lauryl sulfate at *p*H 6.6 (Fig. 4*a*) and uroporphyrin I dissolved in a mixture of pyridine and glycerine (Fig. 4*b*). The cytoplasm of the acinar cells of the Harderian gland of rats has been found to emit strong yet rapidly fading red fluorescence upon excitation with 4070-Å (mercury) light; the presence of protoporphyrin was demonstrated in 55 seconds, with a minimum of fading (Fig. 4*c*). Barely visible red fluorescence has been seen in a fresh frozen section of the duodenal epithelium of a mouse fed with griseofulvin; fluorescence analysis *in situ* with the apparatus indicated that protoporphyrin was present in the cytoplasm (Fig. 4*d; 20*). The accumulation of the porphyrin in liver cells after injection of coproporphyrin has been demonstrated in a cytoplasmic area of 5 by 2 microns (Fig. 4*e*). Figure 4*f* shows the spectrum of a Neon Glow Lamp GE No. 48 recorded with same slit width as that used in Fig. 4*e*. A slight distortion of the peaks of the neon lines, not apparent in Fig. 4*f*, can be seen on the original chart recording (Fig. 4*g*). The distortion is introduced by the pen response time of the recorder at hand for the apparatus. The error thus introduced is about −3 Å. At scanning rates of less than 12 Å/sec, this error is absent for line spectra. However, in band emissions this distortion is never present.

The material presented in Fig. 4 demonstrates that the apparatus provides significant results on tissue structures *in situ* which are not obtainable by any other method. The instrument has been in use in our laboratory for about a year and has routinely produced results comparable to those given in Fig. 4 (*20*). The introduction of a paralleltuned inductance-capacitance plate load in a photomultiplier measuring circuit operating at very low light levels has resulted in a very sensitive device with an adequate signal-to-noise ratio. Other extensions are being added which will permit measurement of spectrophotometric absorption and quantitative analysis of fluorescence spectra. Its usefulness is not limited to the porphyrins.

Summary

A recording photoelectric microfluorospectrophotometer for very low light levels as encountered in tissue-autofluorescence was developed with special reference to detection and identification of cellular porphyrins. The instrument incorporates a tuned inductance-capacitance photomultiplier plate load in conjunction with chopper modulation of the exciting light at 976 cycles per second. The device is sensitive to much less than 10^{-10} gram of protoporphyrin and gives a satisfactory signal-to-noise ratio. Spectral resolution at 6400 Å is less than 20 Å. The spectrum from 5800 to 7030 Å can be scanned in less than a minute.

References and Notes

1. M. Borst and H. Königsdörffer, *Untersuchungen über Porphyrie mit besonderer Berücksichtigung der Porphyria congenita* (S. Hirzel, Leipzig, 1929).
2. C. Casella, *Arch. Biol. Liege* **60**, 207 (1949); B. deLerma, *Boll. Soc. Naturalisti Napoli* **53**, 9 (1942); H. V. Euler, H. Hellström, E. Adler, *Z. Vergleich. Physiol.* **21**, 739 (1935; K. B. Lehmann, *Z. Wiss. Mikroskopie* **30**, 417 (1913); F. Sjöstrand, *Acta Physiol. Scand.* **12**, 42–52 (1946); B. Thorell, in *Porphyrin Biosynthesis and Metabolism*, G. E. W. Wolstenholme and E. C. P. Millar, Eds. (Churchill, London, 1955), pp. 174–182.
3. B. deLerma, in *Handbuch der Histochemie*, W. Graumann and K. H. Neumann, Eds. (Fischer, Stuttgart, 1958), vol. 1.
4. H. Hyden and B. Lindstrom, *Discussions Faraday Soc.* **9**, 436 (1950).
5. S. Schwartz, in *Porphyrin Biosynthesis and Metabolism*, G. E. W. Wolstenholme and E. C. P. Millar, Eds. (Churchill, London, 1955), pp. 183–184.
6. R. W. Engstrom, *J. Opt. Soc. Am.* **37**, 420 (1947).
7. G. R. Harrison, R. C. Lord, J. R. Loofborrow, *Practical Spectroscopy* (Prentice-Hall, New York, 1948); C. D. Hodgman, R. C. Weast, S. M. Selby, *Handbook of Chemistry and Physics* (Chemical Rubber Publishing Co., Cleveland, Ohio, 1957); J. M. Pettit, *Electronic Switching, Timing and Pulse Circuits* (McGraw-Hill, New York, 1959); P. Pringsheim, *Fluorescence and Phosphorescence* (Interscience, New York, 1949); Radio Corp. of America, "Special Red Tubes Nos. 5691–93" (1948); W. J. Runge, in *Human Chromosome Methodology*, J. Yunis, Ed. (Academic Press, New York, 1965); J. Sharpe and E. E. Thomson, "Photomultiplier Tubes and Scintillation Counters" (Document Ref. No. C.P., EMI Electronics Ltd., Hayes, England, 1958); H. Voorhoeve, *Niederfrequenzverstärkertechnik* (Philips Techn. Bibliothek, Eindhoven, 1949); A. A. Xarkevich, *Spektri i Analiz* (Gosudarstvennoe Izdatelstbo Texniko-Teoreticheskoi Literatura, Moscow, 1953).
8. R. W. Landee, D. C. Davis, A. P. Albrecht, *Electronic Designers Handbook* (McGraw-Hill, New York, 1954).
9. R. T. Bruss, unpublished (1950).
10. Obtained as a personal courtesy of Dr. K. Weber and Ernst-Leitz-Werke, Wetzlar, to W. J. Runge (1959).
11. Optische Werke C. A. Steinheil Söhne G.m.b.H., München, "Beschreibung zum Mikrospektroskop" (not dated).
12. W. G. Fastie and H. M. Crosswhite, *J. Opt. Soc. Am.* **46**, 110 (1956).
13. I. A. Greenwood, Jr., J. V. Moldam, Jr., D. McRae, Jr., in vol. 21, *Electronic Instruments*, M.I.T. Radiation Laboratories Series, L. N. Ridenour, Ed. (McGraw-Hill, New York, 1948), p. 565, Figs. 16 to 18.
14. Knight 30 W. Amplifier model #93SZ682, Allied Radio, Chicago, Illinois (1954).
15. H. Rjosk, private communication (1954); J. Runge, private communication (1954).
16. W. J. Runge and L. P. Christenson, unpublished (1959).
17. G. R. Price, unpublished (1956).
18. C. O'h Eocha, *Biochemistry* **2**, 375 (1963).
19. J. N. Phillips, in *Current Trends in Heterocyclic Chemistry*, A. Albert, G. M. Badger, C. W. Shoppe, Eds. (Butterworth, London, 1958), p. 30.
20. F. De Matteis, A. J. Donnelly, W. J. Runge, *Cancer Res.*, in press.
21. Oscar Schott Co., 500 11th Ave. So., Minneapolis, Minnesota. Manufactured as special design #3412 (1963).
22. This work was suported by USPHS grants C-2722, A-4435, and A-2096, by Contract DA-49-193-MD-2296, Research and Development Command, Surgeon General's Office, U.S. Army, and by USAEC contract AT(11-1)108. I thank Drs. C. J. Watson and S. Schwartz for advice and encouragement, L. P. Christenson for assistance, and D. B. McIntyre for construction of the mechanical assembly and suggestions in relation to mechanical problems.